

Vertically well-aligned epitaxial Ni₃₁Si₁₂ nanowire arrays with excellent field emission properties

Chung-Yang Lee, Ming-Pei Lu, Kao-Feng Liao, Wen-Wei Wu, and Lih-Juann Chen

Citation: *Applied Physics Letters* **93**, 113109 (2008); doi: 10.1063/1.2981703

View online: <http://dx.doi.org/10.1063/1.2981703>

View Table of Contents: <http://scitation.aip.org/content/aip/journal/apl/93/11?ver=pdfcov>

Published by the [AIP Publishing](#)

Articles you may be interested in

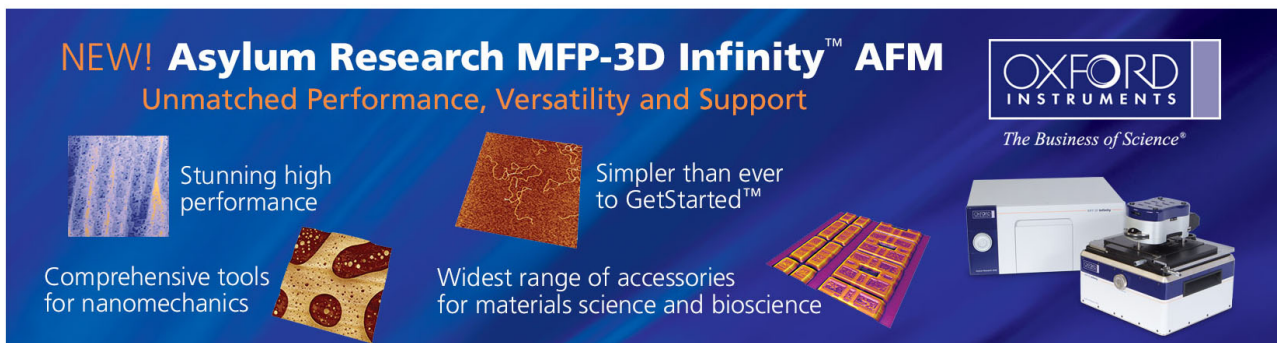
[Epitaxial growth of Ni \(Al \) Si_{0.7} Ge_{0.3} on Si_{0.7} Ge_{0.3} / Si \(100 \) by Al interlayer mediated epitaxy](#)
Appl. Phys. Lett. **98**, 252101 (2011); 10.1063/1.3601464

[Improving field-emission uniformity of large-area W₁₈O₄₉ nanowire films by electrical treatment](#)
J. Vac. Sci. Technol. B **27**, 2420 (2009); 10.1116/1.3263257

[In situ synthesis of In₂O₃ nanowires with different diameters from indium film](#)
Appl. Phys. Lett. **88**, 193119 (2006); 10.1063/1.2202192

[Synthesis and characterization of metallic TaSi₂ nanowires](#)
Appl. Phys. Lett. **87**, 223113 (2005); 10.1063/1.2132523

[Epitaxial growth of Ni₃₁Si₁₂ on \(001\)Si inside nanoscale contact holes prepared by atomic force microscope tip-induced local oxidation of the thin Si₃N₄ layer](#)
J. Vac. Sci. Technol. B **23**, 1905 (2005); 10.1116/1.2000967

The advertisement features a dark blue background with white and orange text. At the top left, it reads 'NEW! Asylum Research MFP-3D Infinity™ AFM' in large white letters, with 'Unmatched Performance, Versatility and Support' in orange below it. The Oxford Instruments logo, consisting of the word 'OXFORD' above 'INSTRUMENTS' in a white box, is in the top right, with the tagline 'The Business of Science®' underneath. The central part of the ad is divided into four quadrants by diagonal lines. The top-left quadrant shows a blue and white textured surface with the text 'Stunning high performance'. The top-right quadrant shows a brown, textured surface with the text 'Simpler than ever to GetStarted™'. The bottom-left quadrant shows a yellow and brown textured surface with the text 'Comprehensive tools for nanomechanics'. The bottom-right quadrant shows a yellow and brown textured surface with the text 'Widest range of accessories for materials science and bioscience'. In the bottom right corner, there is an image of the MFP-3D Infinity AFM instrument, which is a white and blue device with a large lens and a sample stage.

Vertically well-aligned epitaxial Ni₃₁Si₁₂ nanowire arrays with excellent field emission properties

Chung-Yang Lee,¹ Ming-Pei Lu,² Kao-Feng Liao,¹ Wen-Wei Wu,³ and Lih-Juann Chen^{1,a)}

¹Department of Material Science and Engineering, National Tsing Hua University, Hsinchu, Taiwan 30013, Republic of China

²National Nano Device Laboratories, Hsinchu, Taiwan 30078, Republic of China

³Department of Material Science and Engineering, National Chiao Tung University, Hsinchu, Taiwan 30010, Republic of China

(Received 28 July 2008; accepted 25 August 2008; published online 18 September 2008)

Vertically well-aligned single crystal Ni₃₁Si₁₂ nanowire (NW) arrays were epitaxially grown on Ni₃₁Si₁₂ films preferentially formed on Ni foil substrates with a simple vapor phase deposition method in one step. The Ni₃₁Si₁₂ NWs are several micrometers in length and 50–80 nm in diameter. The resistivities of the Ni₃₁Si₁₂ NWs were measured to be 51 $\mu\Omega$ cm by four-terminal electrical measurement. The NWs can carry very high currents and possess excellent field emission properties. The growth of vertically well-aligned Ni₃₁Si₁₂ NW arrays shall lead to significant advantages in the fabrication of vertical Si nanodevices. © 2008 American Institute of Physics.

[DOI: 10.1063/1.2981703]

As the microelectronic devices entering into nanoera, the requirements of the metallization in complementary metal oxide semiconductor (MOS) device integration are important to develop new approach for future applications.^{1–5} Among metal silicides, the low resistivity NiSi is currently the most promising material because of its electrical properties and appropriate work function. On the other hand, Ni-rich silicides, such as Ni₂Si and Ni₃₁Si₁₂, have gained much attention for use in fully silicided gates because of their higher work functions (~ 4.8 eV) which can effectively improve the *p*-type MOS device performance.⁶

Nanotechnology has been considered to be one of the most important enabling technologies for the future generation devices. Several growth methods have been adopted to form vertical nickel silicide nanowires (NWs). Freestanding NiSi NWs were first synthesized from chemical vapor deposition process by Decker *et al.*⁷ Wu *et al.*⁸ coated evaporated nickel film onto freestanding silicon NWs to form NiSi with an annealing process. In addition, NiSi,^{7,9,10} Ni₂Si,^{11,12} Ni₃₁Si₁₂,¹³ and Ni₃Si¹⁴ NWs were synthesized by pyrolysis of silane gas,^{7,10,11,13} sputtering silicon onto Ni surfaces⁹ by metal-induced growth (MIG) or using iodine as transport reagent in chemical vapor transport methods.^{12,14} Recently, a new method by nanocontact reaction between Ni and Si NWs to form NiSi NWs¹⁵ has been reported. In addition, Ni silicide NWs were obtained by means of solid-state reactions of the Si NWs with subsequently deposited Ni films.¹⁶

The vertical metal silicide NWs are grown almost exclusively in a random fashion. Oriented growth of NiSi NWs was achieved only with the MIG method on Ni film coated on SiO₂ layer. The growth of 1–2 μ m NWs was induced during the sputtering of Si. However, the growth mechanism was not elucidated.⁹ In the present work, vertically well-aligned Ni₃₁Si₁₂ NW arrays of more than 7 μ m in length were grown. It is worthwhile to mention that self-assembled epitaxial metal silicide NWs on the silicon surface have been extensively investigated.¹

Pure Ni foils (99.9% purity), cleaned in acetone, de-ionized water, hexane, and dilute HNO₃, consecutively, were used as the substrates. After the cleaning process, the Ni foils were placed in an alumina boat and inserted into a quartz tube furnace pumped down to about 1.0×10^{-5} torr in pressure. The flows of 100 SCCM (SCCM denotes cubic centimeter per minute at STP) Ar and 25 SCCM H₂ were kept constant and introduced as the carrier gas with the pressure in the quartz tube fixed at 1 torr. The upstream and downstream ends of the furnace were heated from room temperature to reach 1100 and 750 °C, respectively. Silicon powders (99.9%) in an alumina boat were positioned at the 1100 °C zone upstream in the quartz tube as the source. Ni foils were located downstream at the end of 750 °C zone. The reaction time was set to be 3 h unless otherwise mentioned. The furnace was then allowed to cool down to room temperature.

A field emission scanning electron microscope (FESEM) (JEOL 6500F with an accelerating voltage of 15 kV) was used to examine the morphology of Ni₃₁Si₁₂ NWs. Transmission electron microscopy (TEM) analysis was carried out to verify the crystal structures of NWs in a JEOL JEM 2010 TEM operating at 200 kV. Energy dispersive spectroscopy (EDS) was conducted in the TEM to determine the composition of a single NW. Agilent B1500A semiconductor device analyzer (SDA) with probe station (LakeShore TTP4) and Keithley 4200 SDA with a four-probe inside a FESEM (JEOL 7000F)¹⁷ were used for the electrical measurements.

X-ray diffraction spectra (not shown) of the samples grown at the 750 °C zone indicate that all the diffraction

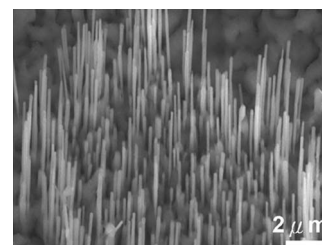


FIG. 1. SEM image of well-aligned Ni₃₁Si₁₂ NW arrays.

^{a)}Electronic mail: ljchen@mx.nthu.edu.tw.

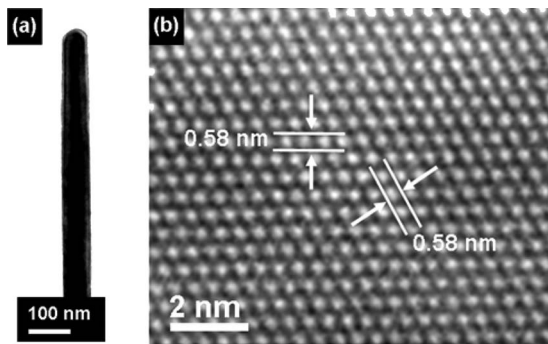


FIG. 2. (a) TEM image of a $\text{Ni}_{31}\text{Si}_{12}$ NW and (b) HRTEM image of the NW after filtering noise.

peaks can be ascribed to hexagonal $\text{Ni}_{31}\text{Si}_{12}$ [space group $P321(150)$, the lattice constants $a=0.6671$ nm and $c=1.2288$ nm (Ref. 18)] NWs and Ni substrate. No diffraction peaks from any other nickel silicide phase and impurities were detected. The diffraction peaks are strong and sharp indicating the high degree of crystallinity of as-grown samples. Figure 1 shows a SEM image of the $\text{Ni}_{31}\text{Si}_{12}$ NWs which were uniformly grown at the 750°C zone on grains of $\text{Ni}_{31}\text{Si}_{12}$ thin film formed on the Ni foil substrate. The length and diameter of $\text{Ni}_{31}\text{Si}_{12}$ NWs are $3\text{--}5\ \mu\text{m}$ and $50\text{--}80$ nm, respectively. As the growth time was prolonged to 6 h, the length and diameter of $\text{Ni}_{31}\text{Si}_{12}$ NWs were increased to $6\text{--}7\ \mu\text{m}$ and $120\text{--}130$ nm, respectively. If the growth temperature was raised to 850°C , vertically aligned Ni_2Si NWs were grown instead.

Figure 2(a) shows TEM image of a single 80 nm $\text{Ni}_{31}\text{Si}_{12}$ NW. The growth direction of $\text{Ni}_{31}\text{Si}_{12}$ NW is $[100]$. High resolution TEM (HRTEM) image in Fig. 2(b) reveals that the NW is single crystalline and defect-free. From the analysis of the EDS spectrum (not shown), the ratio of Ni and Si is close to $2.8:1$.

The cross section TEM image in Fig. 3(a) of a sample prepared with the aid of focused ion-beam (FIB) apparatus and corresponding selected area electron diffraction (SAED) patterns confirms that the NW and underlying film are of the same phase and growth direction of $\text{Ni}_{31}\text{Si}_{12}$. Figure 3(b) shows the cross section TEM image of the $\text{Ni}_{31}\text{Si}_{12}/\text{Ni}$ interface and the corresponding SAED patterns of $\text{Ni}_{31}\text{Si}_{12}$ thin film and Ni substrate. The crystallographic orientation relationships between $\text{Ni}_{31}\text{Si}_{12}$ and Ni are

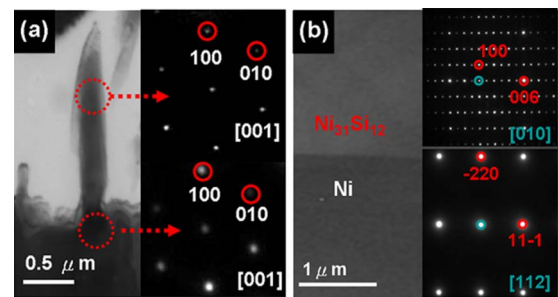


FIG. 3. (Color online) Cross section images of (a) $\text{Ni}_{31}\text{Si}_{12}$ NW and underlying film with the corresponding SAED patterns and (b) $\text{Ni}_{31}\text{Si}_{12}$ film and underlying Ni substrate with the corresponding SAED patterns.

$$[010]\text{Ni}_{31}\text{Si}_{12} \parallel [112]\text{Ni}$$

and

$$(006)\text{Ni}_{31}\text{Si}_{12} \parallel (11-1)\text{Ni}.$$

In Fig. 3(a), the orientation of $\text{Ni}_{31}\text{Si}_{12}$ thin film is (100) . At the $\text{Ni}_{31}\text{Si}_{12}/\text{Ni}$ interface, $\text{Ni}(11-1)$ is parallel to $\text{Ni}_{31}\text{Si}_{12}(006)$ with the interplanar spacings of 0.20344 and 0.2048 nm, respectively, and a small lattice mismatch of 0.66% . Furthermore, in the directions of $\text{Ni}_{31}\text{Si}_{12}[010]$ and $\text{Ni}[112]$ perpendicular to the zone axis, the interplanar spacings are 0.57772 and 0.5756 nm, respectively. The lattice match is as small as 0.47% . Therefore, the $\text{Ni}_{31}\text{Si}_{12}$ NWs and the underlying silicide thin film are well matched to the grains of Ni substrate.

Electrical transport properties of the $\text{Ni}_{31}\text{Si}_{12}$ NWs have been measured by both two- and four-terminal I - V measurements. Pt was deposited as metal contacts with a FIB system¹⁷ on the 500 nm SiO_2 film on Si substrate. From the linear I - V relationship shown in Fig. 4(a), the contacts were found to be Ohmic. The resistivities of the vertical $\text{Ni}_{31}\text{Si}_{12}$ NWs were measured to be 83 and $51\ \mu\Omega\text{cm}$ by two- and four-terminal electrical measurements, respectively. The maximum current density (J_{max}) of $\text{Ni}_{31}\text{Si}_{12}$ NW, obtained by two-terminal measurement as shown in Fig. 4(b), is about $9.8 \times 10^7\ \text{A}/\text{cm}^2$.

For electron FE, NWs are ideal objects because of their special one-dimensional geometry. Figure 5 shows the current density (J) as a function of the applied field (E) in a current density–electric field (J - E) plot and a $\ln(J/E^2)-1/E$ plot of the well-aligned $\text{Ni}_{31}\text{Si}_{12}$ NWs with a $200\ \mu\text{m}$ separa-

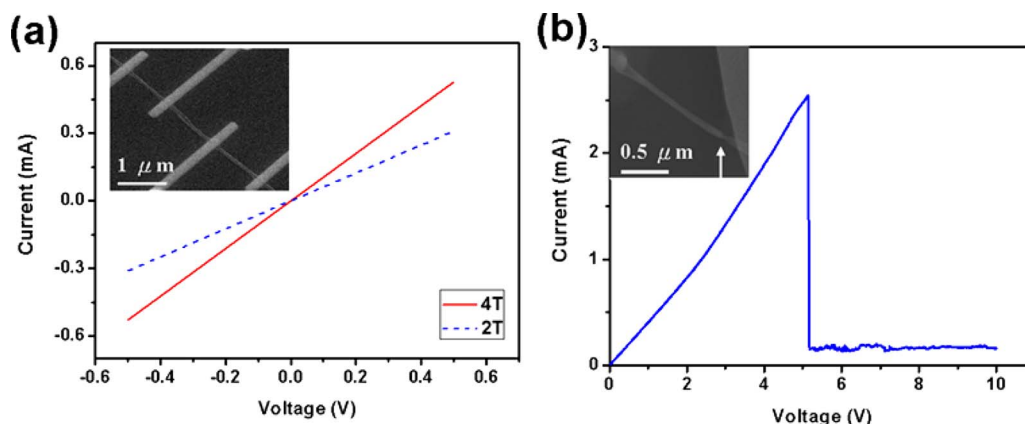


FIG. 4. (Color online) (a) I - V curve of $\text{Ni}_{31}\text{Si}_{12}$ NWs from four-terminal measurement and (b) two-terminal I - V measurement to obtain J_{max} at high applied voltages. Insets show the SEM images of the samples for I - V measurements.

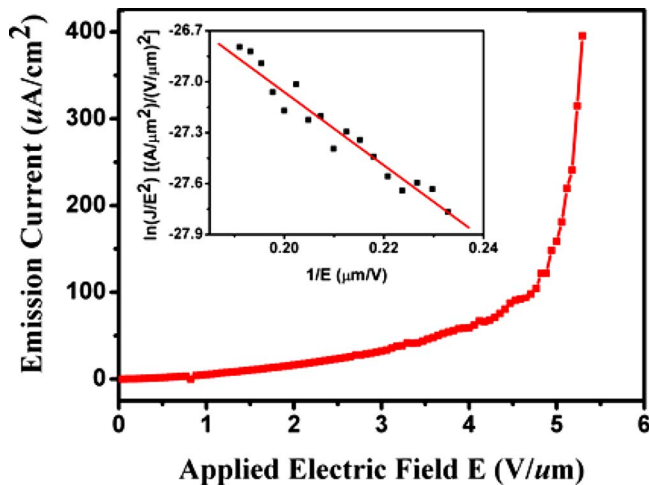


FIG. 5. (Color online) Field-emission curve of $\text{Ni}_{31}\text{Si}_{12}$ NWs as a function of applied electric field. Insets show the corresponding $\ln(J/E^2) - 1/E$ plot.

ration between the anode and emitting surface. The turn-on field was defined as the applied field attained to a current density of $1 \mu\text{A cm}^{-2}$ and was found to be about $1.0 \text{ V } \mu\text{m}^{-1}$. In accordance with the Fowler–Nordheim (FN) relationship, FE current from a metal or semiconductor is attributed to the tunneling of electrons from the material into vacuum through a potential barrier under the influence of an applied field. The FN plot is shown in the inset of Fig. 5. The field enhancement factor β was calculated to be about 3190 for $\text{Ni}_{31}\text{Si}_{12}$ NWs from the slope of the $\ln(J/E^2) - 1/E$ plot with a work function value of about 4.80 eV for $\text{Ni}_{31}\text{Si}_{12}$ NWs.¹⁹ The high FE performance is ascribed to the aligned geometry, especially the long $\text{Ni}_{31}\text{Si}_{12}$ NWs. In addition, epitaxy between Ni silicide NWs, Ni silicide films, and the metal substrates (Ni foil) also assists the electron transport on the side of emitting surface to enhance the FE performance.

The Si vapor from the source zone would react with the substrate of Ni foil to form single crystal Ni silicide ($\text{Ni}_{31}\text{Si}_{12}$) films [Fig. 3(a)] first at the end zone in the furnace. The $\text{Ni}_{31}\text{Si}_{12}$ films would in turn serve as the catalytic surfaces to assist Si vapor to condense and grow $\text{Ni}_{31}\text{Si}_{12}$ NWs epitaxially on thin films.^{20,21} The phase formation of Ni silicides was found to depend on the ratio of Ni and Si.²² Ni atoms are known to be the dominant diffusing species in the Ni–Si reactions.¹⁵ Consequently, Ni atoms from the Ni substrate can be considered as the excess component. As a result, Ni-rich silicide phases (Ni_2Si , $\text{Ni}_{31}\text{Si}_{12}$, and Ni_3Si) are prone to form. On the other hand, the supply of Si vapor would diminish with the distance from the Si source. It correlates well with the finding that Ni_2Si and $\text{Ni}_{31}\text{Si}_{12}$ phases were formed at the zones close and farther away from the source zone downstream, respectively.

The directional growth of NiSi NWs to form nano-bridges over trenches has previously been achieved by the MIG method on Ni film coated on SiO_2 layer. The growth of $1\text{--}2 \mu\text{m}$ NiSi NWs was induced on $1\text{--}3 \mu\text{m}$ Ni grains during the sputtering of Si.⁹ In the present work, vertically well-aligned $\text{Ni}_{31}\text{Si}_{12}$ NW arrays of more than $7 \mu\text{m}$ in length

over $\sim 30 \mu\text{m}$ in diameter areas were grown at the specific temperature zones. The clarification of epitaxial growth mechanism shall further facilitate the practical applications of the grown $\text{Ni}_{31}\text{Si}_{12}$ NWs in nanoelectronics devices.

In summary, vertically well-aligned single crystal $\text{Ni}_{31}\text{Si}_{12}$ NW arrays have been successfully synthesized with a simple vapor transport and condensation method. Highly oriented and large area arrays of NWs were epitaxially grown on $\text{Ni}_{31}\text{Si}_{12}$ films which were in turn preferentially formed on Ni foil substrates at the $750 \text{ }^\circ\text{C}$ zone. The length and width of Ni silicide NWs were found to increase with the growth time. The extent of the growth of NWs is correlated with the size of underlying Ni grains. The NWs can carry very high currents and possess excellent FE properties. The results show that the well-aligned single crystal $\text{Ni}_{31}\text{Si}_{12}$ NWs are potentially useful as high performance field emitters.

The authors would like to acknowledge the support of the ROC National Science Council through Grant Nos. NSC 96-2221-E-007-169-MY3 and NSC 96-2120-M-007-006.

¹L. J. Chen, *JOM* **57**(9), 24 (2005).

²W. M. Weber, L. Geelhaar, A. P. Graham, E. Unger, G. S. Duesberg, M. Liebau, W. Pamlar, C. Cheze, H. Riechert, P. Lugli, and F. Kreupl, *Nano Lett.* **6**, 2660 (2006).

³Y. J. Hu, J. Xiang, G. C. Liang, H. Yan, and C. M. Lieber, *Nano Lett.* **8**, 925 (2008).

⁴S. L. Zhang and M. Ostling, *Crit. Rev. Solid State Mater. Sci.* **28**, 1 (2003).

⁵L. J. Chen, *J. Mater. Chem.* **17**, 4639 (2007).

⁶J. A. Kittl, A. Lauwers, A. Veloso, T. Hoffmann, S. Kubicek, M. Niwa, M. J. H. van Dal, M. A. Pawlak, S. Brus, C. Demeurisse, C. Vrancken, P. Absil, and S. Biesemans, *IEEE Electron Device Lett.* **27**, 966 (2006).

⁷C. A. Decker, R. Solanki, J. L. Freeouf, J. R. Carruthers, and D. R. Evans, *Appl. Phys. Lett.* **84**, 1389 (2004).

⁸Y. Wu, J. Xiang, C. Yang, W. Lu, and C. M. Lieber, *Nature (London)* **430**, 61 (2004).

⁹J. Kim, W. A. Anderson, Y. J. Song, and G. B. Kim, *Appl. Phys. Lett.* **86**, 253101 (2005).

¹⁰C. J. Kim, K. Kang, Y. S. Woo, K. G. Ryu, H. Moon, J. M. Kim, D. S. Zang, and M. H. Jo, *Adv. Mater. (Weinheim, Ger.)* **19**, 3637 (2007).

¹¹X. Q. Yan, H. J. Yuan, J. X. Wang, D. F. Liu, Z. P. Zhou, Y. Gao, L. Song, L. F. Liu, W. Y. Zhou, G. Wang, and S. S. Xie, *Appl. Phys. A: Mater. Sci. Process.* **79**, 1853 (2004).

¹²Y. P. Song, A. L. Schmitt, and S. Jin, *Nano Lett.* **7**, 965 (2007).

¹³J. Kim, D. H. Shin, E. S. Lee, C. S. Han, and Y. C. Park, *Appl. Phys. Lett.* **90**, 253103 (2007).

¹⁴Y. P. Song and S. Jin, *Appl. Phys. Lett.* **90**, 173122 (2007).

¹⁵K. C. Lu, W. W. Wu, H. W. Wu, C. M. Tanner, J. P. Chang, L. J. Chen, and K. N. Tu, *Nano Lett.* **7**, 2389 (2007).

¹⁶Z. Zhang, P. E. Hellstrom, M. Ostling, S. L. Zhang, and J. Lu, *Appl. Phys. Lett.* **88**, 043104 (2006).

¹⁷C. L. Hsin, J. H. He, C. Y. Lee, W. W. Wu, P. H. Yeh, L. J. Chen, and Z. L. Wang, *Nano Lett.* **7**, 1799 (2007).

¹⁸JCPDS Card No. 71-0638.

¹⁹J. A. Kittl, M. A. Pawlak, A. Lauwers, C. Demeurisse, K. Opsomer, K. G. Anil, C. Vrancken, M. J. H. van Dal, A. Veloso, S. Kubicek, P. Absil, K. Maex, and S. Biesemans, *IEEE Electron Device Lett.* **27**, 34 (2006).

²⁰Y. L. Chueh, L. J. Chou, S. L. Cheng, L. J. Chen, C. J. Tsai, C. M. Hsu, and S. C. Kung, *Appl. Phys. Lett.* **87**, 223113 (2005).

²¹Y. L. Chueh, M. T. Ko, L. J. Chou, L. J. Chen, C. S. Wu, and C. D. Chen, *Nano Lett.* **6**, 1637 (2006).

²²C. Y. Kang, P. Lysaght, R. Choi, B. H. Lee, S. J. Rhee, C. H. Choi, M. S. Akbar, and J. C. Lee, *Appl. Phys. Lett.* **86**, 222906 (2005).